レーザー線幅について

2012.6.13　ランチミーティング

担当：鳥井

ELSEVIER

Optics Communications 201 (2002) 391–397

www.elsevier.com/locate/optcom

Frequency noise characterisation of narrow linewidth diode lasers

L.D. Turner, K.P. Weber, C.J. Hawthorn, R.E. Scholten *

School of Physics, University of Melbourne, Parkville, Vic. 3010, Australia

Received 4 October 2001; received in revised form 4 October 2001; accepted 15 November 2001

Abstract

We examine several approaches to laser frequency noise measurement in the frequency and time domains. Commonly employed methods such as optical frequency discrimination and the Allan variance are found to be complex, expensive, time-consuming, or incomplete. We describe a practical method of demodulating a laser beat note to measure a frequency noise spectrum, using a phase-locked loop frequency discriminator based on a single low-cost integrated circuit. This method measures the frequency noise spectrum of a laser directly and in detail and is insensitive to intensity fluctuations. The advantages of this scheme are demonstrated through measurement of the frequency noise spectrum for two external cavity diode lasers (ECDL), clearly distinguishing several common noise sources. These are isolated and removed, reducing the individual laser rms linewidth from 2 MHz to 450 kHz. The spectrum is used to calculate the Allan variance, which shows almost none of the important information. © 2002 Elsevier Science B.V. All rights reserved.

3. Analysis of radio frequency spectra

Frequency noise analysis of the beat signal can provide this information, either in the frequency domain or in the time domain. The beat note signal produced by lasers with frequency difference ν_0 has voltage

$$V(t) = V_0(t)\sin[2\pi\nu_0 + \phi(t)], \quad (1)$$

where $V_0(t)$ describes amplitude fluctuations of the two lasers and $\phi(t)$ is the difference of the individual phases. The instantaneous beat frequency is

$$\nu(t) = \nu_0 + \frac{1}{2\pi}\frac{\mathrm{d}\phi(t)}{\mathrm{d}t} = \nu_0 + \Delta\nu(t) \quad (2)$$

with frequency fluctuations $\Delta\nu(t) \ll \nu_0$.

3.1. Time domain frequency analysis

The time domain parameters are variances of multiple measurements of the instantaneous frequency $\nu(t)$ each of period τ. The standard measure is the Allan variance, the zero dead-time two-sample deviation over a given time period τ:

$$\sigma^2(\tau) = \frac{1}{2}\left\langle [\nu_\tau(t) - \nu_\tau(t+\tau)]^2 \right\rangle, \quad (3)$$

where the brackets $\langle\rangle$ denote time averaging. The measurement of an Allan variance requires two frequency counters, a pulse sequencer, and a computer with data acquisition system to calculate the variance at each time interval [8].

3.2. Frequency domain analysis

The fundamental parameter in the frequency domain is the frequency noise power spectral density, measured in $\mathrm{Hz}^2/\mathrm{Hz}$, given by

$$S_{\Delta\nu}(f) = 2\int_0^\infty \langle \Delta\nu(t)\Delta\nu(t+\tau)\rangle \exp(-\mathrm{i}2\pi f\tau)\,\mathrm{d}\tau, \quad (4)$$

where f is termed the Fourier frequency. The root mean square (rms) linewidth $\Delta\nu_{\mathrm{rms}}$ is then

$$\Delta\nu_{\mathrm{rms}}^2 = \int_0^\infty S_{\Delta\nu}(f)\,\mathrm{d}f. \quad (5)$$

The beat note linewidth measured on an rf spectrum analyser is not simply related to the rms linewidth. If the frequency noise spectrum is a delta function, the rf beat spectrum will be approximately rectangular with width of $L = 2\sqrt{2}\Delta\nu_{\mathrm{rms}}$. If the rf beat spectrum is Gaussian, the full width at half maximum (FWHM) will be $2.35\Delta\nu_{\mathrm{rms}}$ [9].

The Allan variance may be determined from the frequency noise spectrum $S_{\Delta\nu}$ by the integral [10]

$$\sigma^2(\tau) = 2\int_0^\infty S_{\Delta\nu}(f)\frac{\sin^4(\pi f\tau)}{(\pi f\tau)^2}\,\mathrm{d}f \quad (6)$$

but in general *the frequency noise spectrum cannot be determined from the Allan variance* [11]. The frequency noise spectrum is therefore preferable to the Allan variance.

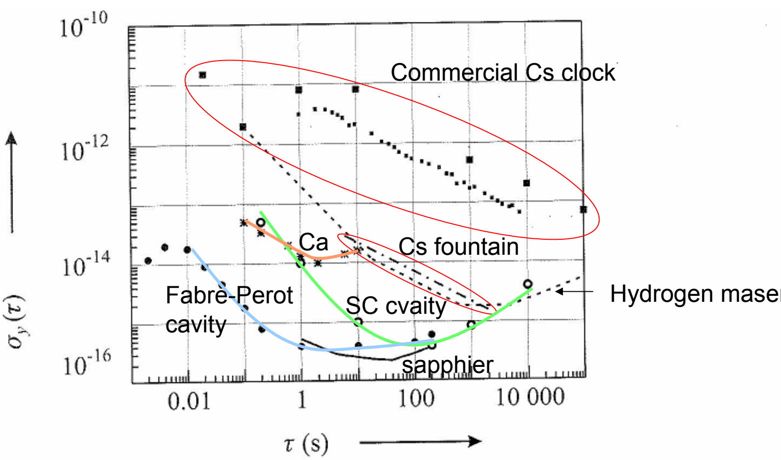

Figure 3.3: Allan deviation $\sigma_y(\tau)$ as a function of the measuring time τ for various highly stable oscillators used as frequency standards and discussed in this book: commercial caesium atomic clock (big squares: [28], small squares: [29]), hydrogen maser (typical, dashed line; see also Fig. 8.5), caesium fountain (dashed dotted line) [18], sapphire loaded cavity microwave-oscillator (thick line) [30], superconducting-cavity stabilised microwave oscillator (open circles [30], laser stabilised to a Fabry–Pérot cavity (full circles) [31], Ca stabilised laser (asterisks)

Riehle, Frequency Standards, p52

Table 3.1: Model of a power law of the power spectral density of fractional frequency fluctuations $S_y(f) = h_\alpha f^\alpha$ and the corresponding power spectral density of phase fluctuations $S_\phi(f)$. The corresponding Allan variance $\sigma_y^2(\tau)$ derived in Section 3.3 holds for a low-pass filter with cut-off frequency f_h when $2\pi f_h \tau \gg 1$.

$S_y(f)$	$S_\phi(f)$	Type of noise	$\sigma_y^2(\tau)$
$h_{-2}f^{-2}$	$\nu_0^2 h_{-2} f^{-4}$	Random walk of frequency noise	$(2\pi^2 h_{-2}/3)\tau^{+1}$
$h_{-1}f^{-1}$	$\nu_0^2 h_{-1} f^{-3}$	Flicker frequency noise	$2h_{-1}\ln 2\tau^0$
$h_0 f^0$	$\nu_0^2 h_0 f^{-2}$	White frequency noise (Random walk of phase noise)	$(h_0/2)\tau^{-1}$
$h_1 f$	$\nu_0^2 h_1 f^{-1}$	Flicker phase noise	$h_1[1.038 + 3\ln(2\pi f_h \tau)]/(4\pi^2)\tau^{-2}$
$h_2 f^2$	$\nu_0^2 h_2 f^0$	White phase noise	$[3h_2 f_h/(4\pi^2)]\tau^{-2}$

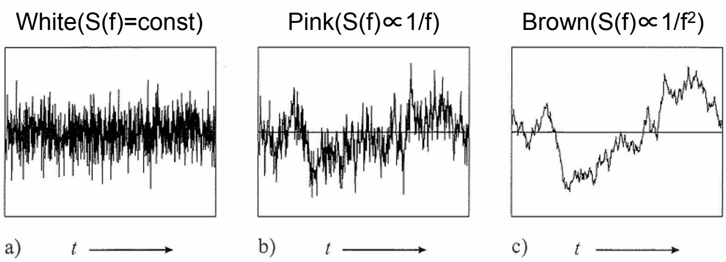

Figure 3.8: Time-domain signal with a) white frequency noise. b) $1/f$ noise. c) $1/f^2$ noise.

Riehle, Frequency Standards, p59

ビート信号のパワースペクトル

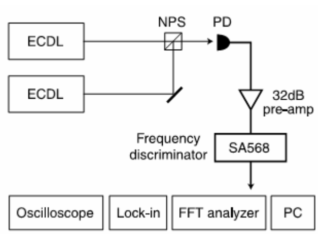

Fig. 1. Two external cavity diode lasers (ECDLs), locked to saturated absorption resonances, were superimposed with a non-polarising beamsplitter (NPS) onto a fast photodiode (PD). The heterodyne signal was pre-amplified and analysed with a frequency discriminator (Philips SA568) and the frequency spectrum acquired with any one of the audio frequency spectrum analysers shown.

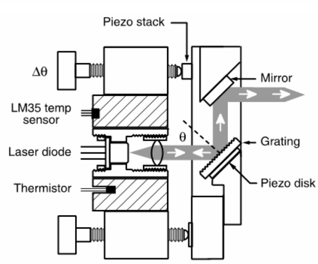

Fig. 2. External cavity diode laser design, based on [15]. An

（注）$S_{\Delta\nu}(f)$ではない！

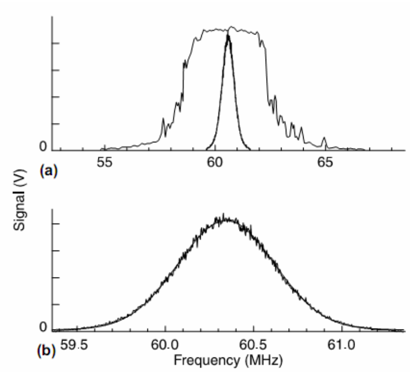

Fig. 3. (a) Beatnote spectra for two ECDLs locked to Rb transitions at 780 nm, separated by 60.3 MHz, before and after noise minimisation modifications. (b) Detail of the beatnote spectrum after noise minimisation modifications, taken with 3 kHz resolution bandwidth, averaged over 64 sweeps of 2 s each. The close agreement with a Gaussian fit (smooth curve) indicates that the deviations in laser frequency are large compared to the frequencies of modulation [9].

アラン分散と周波数ノイズスペクトルの比較

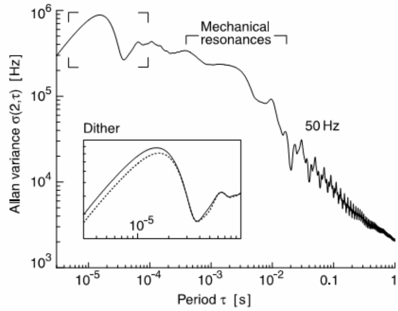

Fig. 5. Allan variance calculated from frequency noise data in Fig. 4. The inset shows an expanded view with an added curve (dashed) calculated from a frequency noise spectrum from which the higher frequency dither peak has been deleted (···). The two variances are almost indistinguishable, whereas in Fig. 4 the dither peaks are clearly resolved.

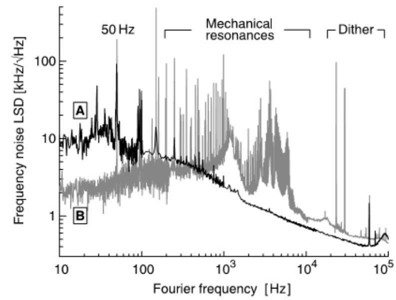

Fig. 4. Frequency noise linear spectral density (the square-root of the power spectral density $S_{\Delta\nu}(f)$) of ECDL beat note, before (B) and after (A) noise minimisation modifications.

Gaussian or Lorenzian?

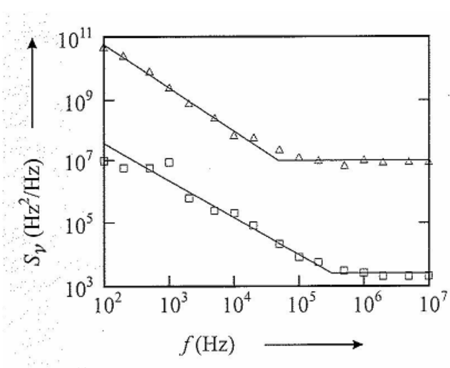

$S_\nu(f_c)/f_c >> 1 \rightarrow$ Lorenzian lineshape

$S_\nu(f_c)/f_c << 1 \rightarrow$ Gaussian lineshape

この論文の条件はこっち

Figure 3.10: Measured power spectral densities of frequency fluctuations versus Fourier frequency f of a diode laser without optical feedback (triangles) and with optical feedback from a grating (squares) after [40] with permission.

Riehle, Frequency Standards, p67

レーザー線幅について(つづき)

2012.6.20　ランチミーティング

担当:鳥井

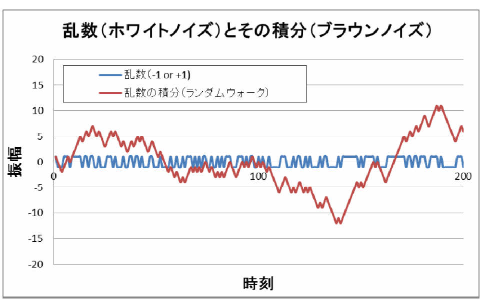

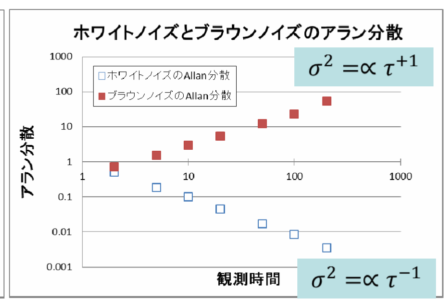

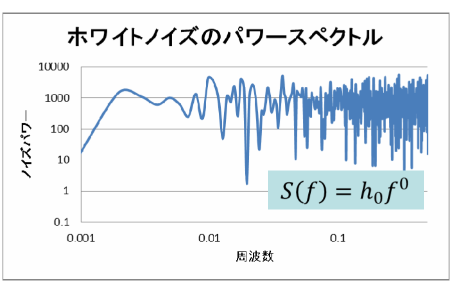

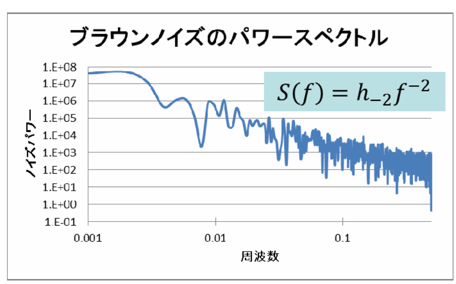

Table 3.1: Model of a power law of the power spectral density of fractional frequency fluctuations $S_y(f) = h_\alpha f^\alpha$ and the corresponding power spectral density of phase fluctuations $S_\phi(f)$. The corresponding Allan variance $\sigma_y^2(\tau)$ derived in Section 3.3 holds for a low-pass filter with cut-off frequency f_h when $2\pi f_h \tau \gg 1$.

$S_y(f)$	$S_\phi(f)$	Type of noise	$\sigma_y^2(\tau)$
$h_{-2}f^{-2}$	$\nu_0^2 h_{-2} f^{-4}$	Random walk of frequency noise	$(2\pi^2 h_{-2}/3)\tau^{+1}$
$h_{-1}f^{-1}$	$\nu_0^2 h_{-1} f^{-3}$	Flicker frequency noise	$2h_{-1}\ln 2\tau^0$
$h_0 f^0$	$\nu_0^2 h_0 f^{-2}$	White frequency noise (Random walk of phase noise) （注）位相のランダムウォークは周波数のホワイトノイズ	$(h_0/2)\tau^{-1}$
$h_1 f$	$\nu_0^2 h_1 f^{-1}$	Flicker phase noise	$h_1[1.038 + 3\ln(2\pi f_h \tau)]/(4\pi^2)\tau^{-2}$
$h_2 f^2$	$\nu_0^2 h_2 f^0$	White phase noise	$[3h_2 f_h/(4\pi^2)]\tau^{-2}$

環境のドリフト？

メカニカルノイズ？
注入電流ノイズ？

Schawlow-Townes
の線幅（intrinsic）

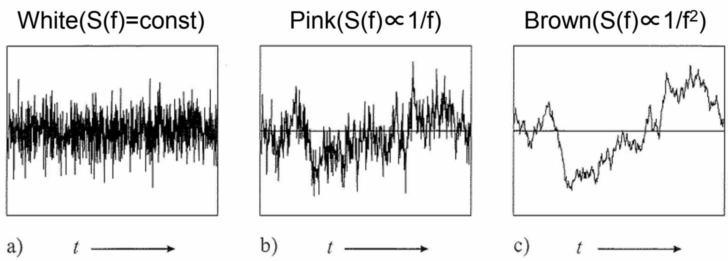

Figure 3.8: Time-domain signal with a) white frequency noise. b) $1/f$ noise. c) $1/f^2$ noise.

Riehle, Frequency Standards, p59

技 術 資 料

光格子時計のための線幅 1 Hz級レーザーの開発

保坂 一元*

（平成20年2月13日受理）

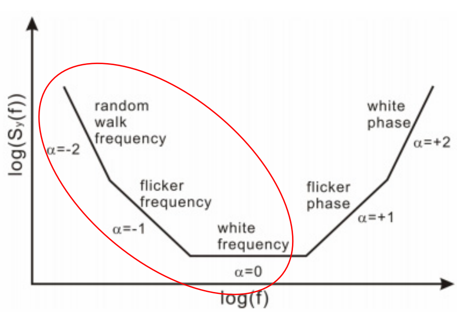

図1　典型的な雑音のスペクトル密度

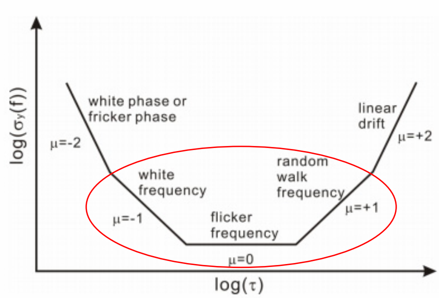

図2　典型的な雑音のアラン分散

自然放出で決まるレーザー周波数線幅（Schawlow-Townes線幅）

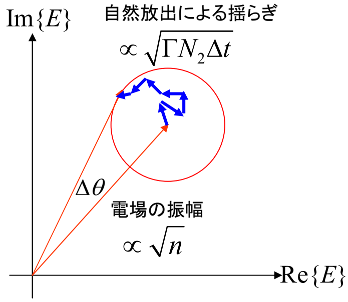

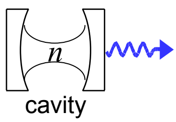

$$P = \frac{\hbar\omega n}{\tau_C}$$

共振器の線幅（FWHM）: $\Delta\omega_C = 1/\tau_C$

基底状態の原子数: N_1

励起状態の原子数: N_2

レート方程式　　誘導放出と吸収

$$\frac{dn}{dt} = -\frac{n}{\tau_C} + \Gamma(N_2 - N_1)n - \Gamma N_2$$

レーザー出力　　自然放出

レーザーのコヒーレンス時間をΔt_cとすると

$$\Delta\theta = \frac{\sqrt{\Gamma N_2 \Delta t_c}}{\sqrt{n}} \sim 1$$

n>>1の定常状態を仮定すると、

$$\Delta\omega = \frac{1}{\Delta t_c} = \frac{N_2}{N_2 - N_1}\frac{\hbar\omega(\Delta\omega_C)^2}{P}$$

Schawlow-Townesの線幅

Schawlow-Townesの線幅

$$\Delta\omega = \frac{\hbar\omega_0(\Delta\omega_C)^2\mu}{P} \quad \left(\Delta\nu = \frac{2\pi\nu_0(\Delta\nu_{1/2})^2\mu}{P}\right)$$

$$\Delta\omega_C = 2\pi\Delta\nu_{1/2} = 1/\tau_C,\ \mu = \frac{N_2}{N_2 - N_1}$$

半導体レーザーの場合、レーザーの強度揺らぎが、屈折率揺らぎを引き起こし、これがレーザーの位相揺らぎを引き起こすため、一般にこれより大きくなる。

$$\Delta\omega = \frac{\hbar\omega_0(\Delta\omega_C)^2\mu}{P}(1+\alpha^2)$$

$$(\alpha \equiv \Delta n' / \Delta n'' = 4 \sim 8)$$

屈折率の実部と虚部の比

C. Henry, IEEE J. QE18, 259 (1982)

20 December 2006 / Vol. 45, No. 36 / APPLIED OPTICS 9191

Influence of grating parameters on the linewidths of external-cavity diode lasers

Huanqian Loh, Yu-Ju Lin, Igor Teper, Marko Cetina, Jonathan Simon, James K. Thompson, and Vladan Vuletić

We investigate experimentally the influence of the grating reflectivity, grating resolution, and diode facet antireflection (AR) coating on the intrinsic linewidth of an external-cavity diode laser built with a diffraction grating in a Littrow configuration. Grating lasers at 399, 780, and 852 nm are determined to have typical linewidths between 250 and 600 kHz from measurements of their frequency noise power spectral densities. The linewidths are little affected by the presence of an AR coating on the diode facet but narrow as the grating reflectivity and grating resolution are increased, with the resolution exerting a greater effect. We also use frequency noise measurements to characterize a laser mount with improved mechanical stability. © 2006 Optical Society of America

OCIS codes: 140.2020, 140.3600, 050.1950.

（注）この論文では、周波数ノイズのパワースペクトルの平方根を*S*(*f*)と定義している

3.4.1 Power Spectrum of a Source with White Frequency Noise

We now consider a source whose power spectral density in the Fourier-frequency domain can be represented as white (frequency independent) frequency noise S_ν^0 (see Table 3.1). Consequently,

$$S_\phi(f) = \frac{S_\nu^0}{f^2} = \frac{\nu_0^2 h_0}{f^2} \tag{3.67}$$

holds and the integral in the exponential of (3.66) can be solved analytically using $\int_0^\infty [1 - \cos(bx)]/x^2 dx = \pi|b|/2$ leading to

$$\begin{aligned} S_E(\nu-\nu_0) &= E_0^2 \int_{-\infty}^{\infty} \exp -[i2\pi(\nu-\nu_0)\tau] \exp\left(-\pi^2 h_0 \nu_0^2 |\tau|\right) d\tau \\ &= 2E_0^2 \int_0^{\infty} \exp -\tau\left[i2\pi(\nu-\nu_0) + \pi^2 h_0 \nu_0^2\right] d\tau. \end{aligned} \tag{3.68}$$

Solving the integral (3.68) and keeping the real part leads to the power spectral density of

$$S_E(\nu-\nu_0) = 2E_0^2 \frac{h_0\pi^2\nu_0^2}{h_0^2\pi^4\nu_0^4 + 4\pi^2(\nu-\nu_0)^2} = 2E_0^2 \frac{\gamma/2}{(\gamma/2)^2 + 4\pi^2(\nu-\nu_0)^2} \tag{3.69}$$

with $\gamma \equiv 2h_0\pi^2\nu_0^2 = 2\pi(\pi h_0 \nu_0^2) = 2\pi(\pi S_\nu^0)$. Hence, the power spectral density of frequency fluctuations in the carrier-frequency domain of an oscillator with white frequency noise S_ν^0 in the Fourier-frequency domain, is a Lorentzian whose full width at half maximum is given by

$$\boxed{\Delta\nu_{\mathrm{FWHM}} = \pi S_\nu^0.} \quad \text{←紹介する論文（式(1)）では } \pi S_0^2 \tag{3.70}$$

Similarly, other types of phase noise spectral densities can be calculated accordingly. Godone and Levi have furthermore treated the case of white phase noise and flicker phase noise [38].

Riehle, Frequency Standards, p66

この論文の主張(要点)

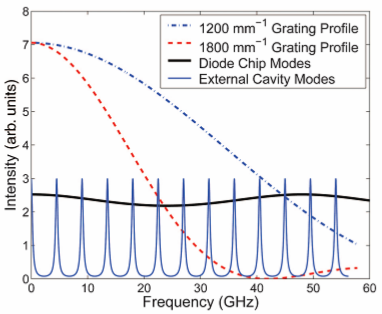

Fig. 4. (Color online) Calculated profiles of 1200 and 1800 mm^{-1} gratings, overlapped with diode-chip modes and external-cavity modes spaced by frequency intervals determined from Fig. 1. The passive external-cavity mode spectrum is calculated for a grating of reflectivity R_{G1} = 0.61 and diode back facet reflectivity R_1 = 0.85. The diode chip mode spectrum is calculated for an AR-coated ($R_2 = 10^{-4}$) diode with a regenerative gain parameterized by the material absorption coefficient α_L = 45 cm^{-1} (Ref. 29).

- レーザー線幅はグレーティングの反射率にはあまり依存しない。
- ARコーティングの有り無しにもあまり依存しない。
- しかしグレーティングの波長分解能には大きく依存する
- レーザー線幅狭窄化には、モード間競合(mode competition)の抑制がより重要である。

マウントA

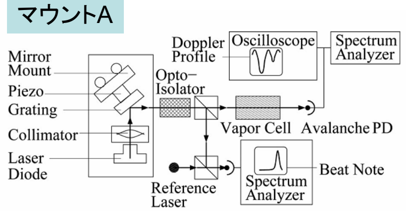

Fig. 2. Schematic of the setup used to measure laser frequency noise. Components such as attenuators are not drawn. The polarization of the laser light is out of the plane.

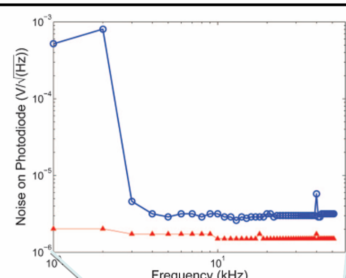

Fig. 3. (Color online) Total (open circles) and amplitude (filled triangles) spectral noise densities of an 852 nm AR-coated laser assembled with a 1200 mm^{-1} grating of reflectivity R_{G1} = 0.21. For the frequency noise, 1 V/$\sqrt{\mathrm{Hz}}$ corresponds to 156 MHz/$\sqrt{\mathrm{Hz}}$. For the amplitude noise, 1 V/$\sqrt{\mathrm{Hz}}$ corresponds to a fractional noise of 0.94/$\sqrt{\mathrm{Hz}}$.

マウントB

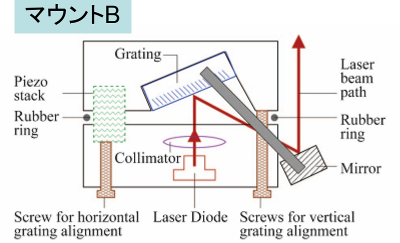

Fig. 6. (Color online) Schematic of mount B. The four nylon pull screws that attach the two aluminum blocks to each other are not drawn.

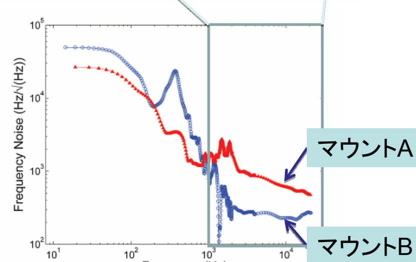

Fig. 7. (Color online) Frequency noise power spectral densities for mount B (open circles) and mount A (filled triangles) lasers. Mount B only has a strong mechanical resonance at 500 Hz, whereas mount A has mechanical resonances at 2 kHz.

Table 2. Linewidths of Both Non-AR- and AR-Coated 780 nm Lasers[a]

Diode Model	L_d (μM)	R_1	R_2	$\Delta\nu_{th}$ (kHz)	$\Delta\nu_{exp}$ (kHz)
Sanyo DL7140-201S	840	0.85	0.15	4900,[b] 130,[c] –[e]	500 ± 80
SAL-780-40	890	0.85	8×10^{-5}	43,000,[b] 260,[c] 370[d]	450 ± 80

[a]Linewidths of 780 nm lasers without and with an AR coating on the diode front facet, assembled with the same grating (Edmund Optics 43773). L_d is the diode chip length, while R_1 and R_2 are the back and front facet power reflectivities, respectively. $\Delta\nu_{th}$ and $\Delta\nu_{exp}$ are as defined in Table 1.
[b]Reference 28.
[c]$\Delta\nu_{th} = \Delta\nu_0/(1 + A + B)^2$, where A and B are calculated from Eq. (26) of Kazarinov and Henry's paper (Ref. 12).
[d]Calculated from Eq. (8) of the paper of Sun *et al.* (Ref. 10).
[e]The calculations of Sun *et al.* do not apply for $R_2/R_{G1} \sim 1$ (Ref. 10).

Table 1. Linewidths of 852 nm Lasers for Different Gratings in the Littrow Configuration[a]

n (mm^{-1})	$\lambda/\Delta\lambda$	R_{G1}	R_{G0}	$\Delta\nu_{th}$ (kHz)	$\Delta\nu_{exp}$ (kHz)
1200	4200	0.21	0.67	260,[b] 290,[c] 320[d]	560 ± 140
1200	4200	0.61	0.19	260,[b] 270,[c] 290[d]	440 ± 110
1800	8400	0.16	0.78	260,[b] 290,[c] 330[d]	320 ± 60

[a]Linewidths of AR-coated 852 nm lasers built with gratings 43773, 43753, 43222 from Edmund Optics for lines 1–3. For a Littrow grating laser, the first diffraction order with power reflectivity R_{G1} is reflected back into the laser for optical feedback, while the zeroth order with power reflectivity R_{G0} is used as the laser output. The grating resolution $\lambda/\Delta\lambda$ is computed for a beam diameter of $D \simeq 3$ mm from the groove density n and the Littrow angle. The free-running laser linewidth is estimated to be 35 MHz (Ref. 28). $\Delta\nu_{th}$ lists different theoretical predictions for the given laser parameters, and $\Delta\nu_{exp}$ is the linewidth measured using Eq. (1).
[b]$\Delta\nu_{th} = \Delta\nu_0[\tau_d/(\tau_d + \tau_e)]^2$.
[c]$\Delta\nu_{th} = \Delta\nu_0/(1 + A + B)^2$, where A and B are calculated from Eq. (26) of Kazarinov and Henry (Ref. 12).
[d]Calculated from Eq. (8) of the paper of Sun *et al.* (Ref. 10).

Table 3. Best Achieved Linewidths[a]

Atoms	λ (nm)	AR Coating	n (mm^{-1})	$\lambda/\Delta\lambda$	R_{G1}	$\Delta\nu_{exp}$ (kHz)
Cs	852	Yes	1800	8400	0.16	320 ± 60
Rb	780	Yes	1200	4100	0.27	450 ± 80
Yb	399	No	2400	8200	0.60	2508 ± 70

[a]Narrowest linewidths achieved with 852 and 780 nm lasers and their corresponding diode and grating parameters as defined in Table 1.

250kHzの間違い

1/fノイズ（メカニカルノイズ）による線幅

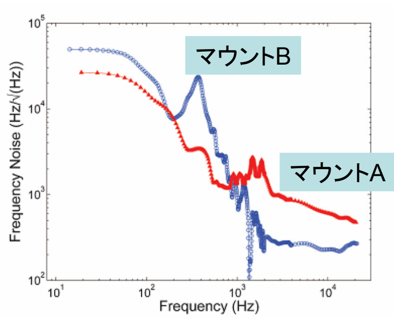

Fig. 7. (Color online) Frequency noise power spectral densities for mount B (open circles) and mount A (filled triangles) lasers. Mount B only has a strong mechanical resonance at 500 Hz, whereas mount A has mechanical resonances at 2 kHz.

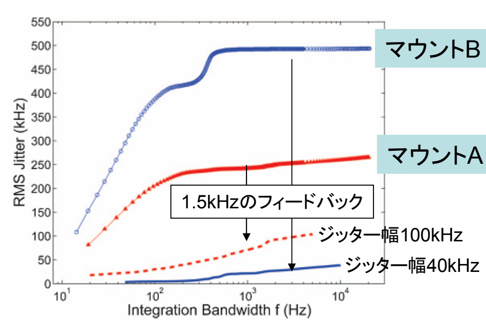

Fig. 8. (Color online) Rms jitters of lasers assembled both with mount B (open circles for unlocked and solid curve for locked) and mount A (filled triangles for unlocked and dashed curve for locked) versus integration bandwidth f. The rms jitter is given by $\boxed{\Delta\nu_{jitter}(f) = [\int_0^f (S(f'))^2 df']^{1/2}.}$

パワースペクトルの積分の平方根が自乗平均幅を与える

一見、マウントAの方がよさそうに見えるが、バンド幅1.5kHzのフォードバックをかけた場合は、マウントBの方が狭い線幅を与える（共振周波数が低いため）。